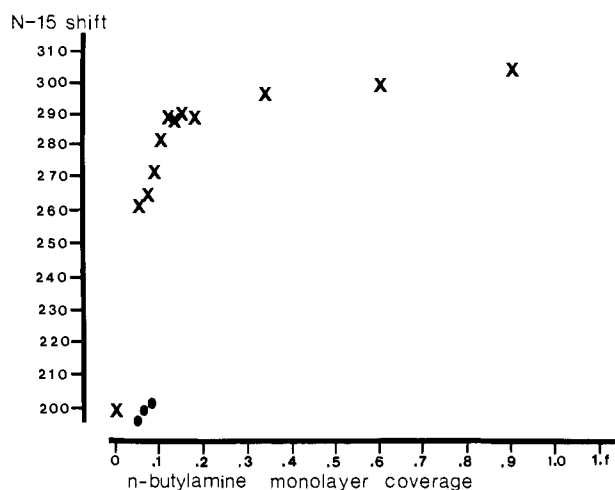


**Figure 1.** 20.3-MHz  $^{15}\text{N}$  CP/MAS NMR spectra of pyridine- $^{15}\text{N}$  (Py) adsorbed on silica-alumina in the presence of varying amounts of *n*-butylamine (NBA); 0.19 mmol Py/g silica-alumina (except for 1a for which 0.17 mmol Py/g silica-alumina); mmoles of Py and NBA adsorbed on Brønsted (B), Lewis (L), and hydrogen-bonding (HB) sites indicated numerically. Typical parameters: 2-ms contact time, 1-s repetition time, and 50 000 scans. Chemical shifts in ppm relative to external liquid ammonia (larger numbers, lower shielding). Mole ratio of *n*-butylamine to pyridine: (a) 0; (b) 0.4; (c) 0.6; (d) 0.8; (e) 1.0; (f) 1.2; (g) 1.4; (h) 1.6; (i) 2.0; (j) 4.0; (k) 7.0; (l) 11.



**Figure 2.** Plot of pyridine  $^{15}\text{N}$  chemical shift as a function of total *n*-butylamine surface coverage. (*n*-Butylamine is assumed to occupy the same surface area as pyridine.) For spectra with two clearly-resolved peaks, X represents the major (most intense) peak and ● represents the minor peak.

used in this study, so the  $^{15}\text{N}$  spectra contain no signals from this compound. Figure 1a is the spectrum obtained on a sample with no added *n*-butylamine. The  $^{15}\text{N}$  chemical shift (198 ppm relative to external liquid ammonia) is characteristic of protonated pyridine,<sup>6,7</sup> indicating that essentially all adsorbed pyridine molecules in this sample are associated with Brønsted acid sites. This observation places a lower limit of roughly 0.17 mmol/g silica-alumina on the concentration of Brønsted acid sites. The two low-intensity signals  $\sim 2$  kHz to either side of the intense signal are at least largely spinning sidebands. The low relative intensity of these sidebands suggests that molecular motion reduces the  $^{15}\text{N}$  powder pattern width substantially (from 782 ppm<sup>11</sup> to less than 400 ppm).

The addition of 0.4–0.8 equiv of *n*-butylamine shifts an increasing fraction of the  $^{15}\text{N}$ -resonance intensity of pyridine to 261–271 ppm (Figures 1b–d). When about 1.0 equiv of *n*-butylamine has been added, the pyridine peak associated with Brønsted acid sites is absent (Figure 1e), so an upper limit of roughly 0.19 mmol/g silica-alumina can be established on the concentration of Brønsted sites (strong enough to protonate pyridine). The lower shielding peaks in the pyridine spectra obtained with *n*-butylamine-to-pyridine mole ratios of 0.4–0.8 (Figures 1b–d) are much broader than the main peak in Figure 1a. This broad peak at about  $265 \pm 5$  ppm is characteristic of pyridine coordinated to a Lewis acid site.<sup>6,7</sup>

Spectra of samples with more than 1 equiv of *n*-butylamine show one relatively sharp signal at 289–303 ppm. A chemical shift of 295 ppm is characteristic of hydrogen-bonded pyridine.<sup>6,7</sup> The use of 11 equiv of *n*-butylamine results in a shift of the pyridine resonance to 303 ppm (Figure 1l), a value intermediate between hydrogen-bonded pyridine and that characteristic of neat (liquid) pyridine. The total concentration of adsorbed amine (pyridine + *n*-butylamine) is 2.28 mmol/g silica-alumina for the sample with a *n*-butylamine-to-pyridine mole ratio of 11. Assuming that *n*-butylamine occupies approximately the same surface area as pyridine allows us to calculate a total amine surface coverage for this sample of 0.98 monolayer. With an *n*-butylamine pressure of 30 torr it was found to be impossible to deposit more than 12 equiv of *n*-butylamine on the surface. The latter two observations suggest that this technique can be used to measure the surface area of silica-alumina.

The strong similarities between the results shown in Figure 1 and those of classical titrations prompted us to cast these data in the form of a titration curve, shown in Figure 2. In this “titration” pyridine serves as the indicator and *n*-butylamine as the titrant.

The line widths and relative intensities of the spectra in Figure 1 show wide variations, which can, we believe, be reconciled in terms of molecular motion. The hydrogen-bonded species are expected to be very mobile and have reduced cross-polarization efficiencies. Lewis acid-base complexation requires orbital overlap, a stringent restriction on molecular mobility. We have observed that pyridine adsorbed at Lewis acid sites yields the strongest CP signals, a result consistent with restricted mobility. Further  $^{15}\text{N}$  NMR studies of these kinds of systems are in progress.

**Acknowledgment.** We are grateful to the National Science Foundation for partial support of this work under Grant CHE-8306518 and to the Colorado State University Regional NMR Center, funded by National Science Foundation Grant CHE-8208821.

**Registry No.** Pyridine, 110-86-1; *n*-butylamine, 109-73-9; silica, 7631-86-9; alumina, 1344-28-1.

(11) Schweitzer, D.; Spiess, H. W. *J. Magn. Reson.* 1974, 15, 529.

## Ethylene Biosynthesis. 2. Stereochemistry of Ripening, Stress, and Model Reactions

Michael C. Pirrung

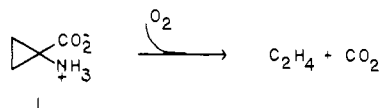
Department of Chemistry, Stanford University  
Stanford, California 94305

Received July 5, 1983

We recently described models for two potential reactive intermediates in the biosynthesis of the plant growth hormone ethylene.<sup>1</sup> Because of the lability of the natural biosynthetic

(1) See paper 1 in this series: Pirrung, M. C.; McGeehan, G. M. *J. Org. Chem.*, in press.

system,<sup>2,3</sup> it has proved difficult to probe the means by which the immediate biosynthetic precursor, aminocyclopropanecarboxylic acid (ACC, **1**), is converted to ethylene. This communication reports the stereochemistry of the conversion of ACC-*d*<sub>2</sub> to ethylene in both natural and model systems and suggests a sequential single-electron-transfer pathway for ethylene biosynthesis.



The preparation of *cis*-ACC-*d*<sub>2</sub> (**1-d**<sub>2</sub>) was accomplished by applying the method of Schöllkopf<sup>4</sup> to *meso*-1,2-dibromo-1,2-dideuterioethane to obtain 1-isocyanocyclopropane-2,3-*d*<sub>2</sub>-carboxylic acid. After basic hydrolysis and ion-exchange chromatography, **1-d**<sub>2</sub> is obtained in 36% overall yield. That it is strictly *cis* was ascertained by <sup>1</sup>H, <sup>2</sup>H, and <sup>13</sup>C NMR spectra,<sup>5</sup> though it is a mixture of diastereomers at the fully substituted cyclopropane carbon.

Compound **1-d**<sub>2</sub> was fed<sup>6</sup> to apple and cantaloupe disks, representing ripening ethylene biosynthesis, and mung bean hypocotyls, representing the stress ethylene response.<sup>8</sup> In all three cases, 1:1 mixts. of *cis*- and *trans*-dideuterioethylenes are produced, as evidenced by signals in the infrared spectrum of the reaction headspace at 842 and 988 cm<sup>-1</sup>, respectively.<sup>9</sup> The result in the apple system has received independent confirmation in Baldwin's laboratory.<sup>10</sup> Control experiments demonstrate that *cis*-dideuterioethylene is stereochemically stable to the incubation conditions.

Because these results imply a stepwise oxidation and no model system for ethylene biosynthesis has yet been described that unambiguously proceeds through such a pathway, the behavior of ACC and related compounds under electrochemical oxidation was examined.

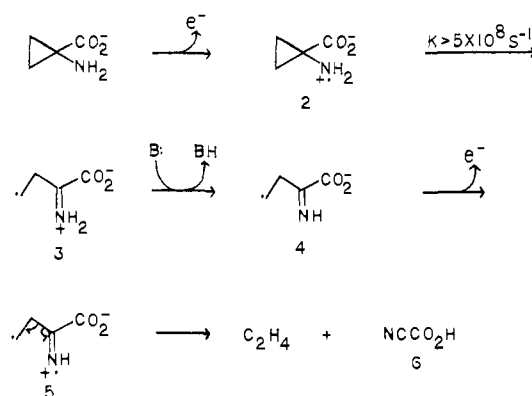
ACC and three related models, cyclopropylamine, cyclopropanecarboxylic acid, and  $\alpha$ -aminoisobutyric acid (AIB), were first examined by cyclic voltammetry.<sup>11</sup> Somewhat surprisingly, cyclopropylamine and cyclopropanecarboxylate are oxidized at quite comparable potentials (ca. +1.1 V vs. SCE). As expected, the oxidations are irreversible.<sup>12</sup> In contrast, ACC carboxylate

and AIB carboxylate are oxidized with readily identified waves at ca. +0.7 V vs. SCE.<sup>13</sup>

The preparative electrolysis of ACC carboxylate was conducted at +0.8 V vs. SCE.<sup>14</sup> Coulometry demonstrates that at limiting current, <sup>2</sup>/<sub>3</sub> F/mol of substrate had been passed.<sup>15</sup> Analysis of the reaction headspace reveals that ACC is converted to ethylene.<sup>16</sup> Plots of ethylene concentration vs. Coulombs passed are linear. Furthermore, analysis of the anolyte shows cyanide ion is formed in the same molar amount as ethylene.<sup>17</sup> Cyclopropylamine is also oxidized (+1.2 V vs. SCE) to give ethylene, albeit in slightly lower yield than in the case of ACC carboxylate. This result suggests that ACC is primarily oxidized at its amino group.

With this electrochemical model for ethylene biosynthesis established, its stereochemistry remained to be determined. Oxidation of ACC-*d*<sub>2</sub> under the electrochemical conditions used above leads to ethylene that is stereochemically scrambled. Control experiments again demonstrate the stability of *cis*-dideuterioethylene to the reaction conditions.

The mechanism for both the natural biosynthetic systems and the electrochemical model system that is suggested by these results is shown below. An initial single-electron oxidation yields **2**, which



is quite analogous to the cyclopropylaminyl radicals investigated by Ingold.<sup>18</sup> These species undergo rapid ring opening. This proposal is analogous to one made by Silverman,<sup>19</sup> Guengerich,<sup>20</sup> and Hanzlik<sup>21</sup> for some enzymatic oxidations of benzyl cyclopropyl amines. Species **3** might also have been foreshadowed by EPR evidence for a "carbon-centered free radical" in other ACC model oxidations.<sup>22</sup> Deprotonation and a second one-electron oxidation

(2) Adams, D.; Yang, S. *Proc. Natl. Acad. Sci. U.S.A.* **1979**, *76*, 170.

(3) Liebermann, M. *Annu. Rev. Plant Physiol.* **1979**, *30*, 533.

(4) Schöllkopf, U.; Harms, R.; Hoppe, D. *Liebigs. Ann. Chem.* **1973**, 611.

(5) <sup>1</sup>H NMR (D<sub>2</sub>O, HOD = 4.80)  $\delta$  1.29 (s, 2 H), 1.16 (s, 2 H); <sup>13</sup>C NMR (D<sub>2</sub>O, internal Me<sub>2</sub>SO = 39.56)  $\delta$  12.2 (1:1:1 triplet, *J* = 25.2); <sup>2</sup>H NMR (H<sub>2</sub>O, HOD = 4.80)  $\delta$  1.21 (s, 2 D), 1.12 (s, 2 D).

(6) A 15–20-g sample of plant material was used. The amino acid (5–15 mg) in 5–10 mL of 2% sucrose was added and the reaction vessel sealed for a 10–24-h incubation in the dark. The concentration of ethylene was monitored via gas chromatography,<sup>7</sup> which proved especially critical in the case of mung bean hypocotyls. The ethylene concentration achieves a maximum at 10–18 h, then declines. Because this system produces much smaller quantities of ethylene than the ripening systems, the ethylene concentration must be as great as possible for effective product analysis.

(7) Ethylene was identified and quantified by gas chromatography using an 80% Porapak N/20% Porapak Q 6 ft  $\times$  1/8 in. column, operated at 35 °C and using flame-ionization detection. This system allows detection of <0.3 ppm ethylene.

(8) When subjected to environmental stress (flooding, wounding, etc.), an ethylene response is induced in a variety of plant tissues. Because the control point for ethylene biosynthesis is at the ACC synthase step and the ethylene-forming enzyme is constitutive, feeding of ACC to tissues which do not utilize a ripening hormone still yields an ethylene response, which is identified as a stress response. Mung bean hypocotyls are commonly used for this purpose; cf.: Yoshii, H.; Watanabe, A.; Imaseki, H. *Plant Cell Physiol.* **1980**, *21*, 279.

(9) Infrared spectra were obtained in a 20-cm path length gas cell with a Nicolet 7199 FTIR operated with a Hg-Cd-Te cooled detector. This arrangement allows 1-cm<sup>-1</sup> spectra to be obtained on as little as 50 ppm of ethylene-*d*<sub>2</sub> in ca. 2000 acquisitions. The spectra are provided in the supplementary material. Note that the extinction coefficient for the *cis* isomer is ca. twice that for the *trans*.

(10) Adlington, R.; Baldwin, J.; Rawlings, B. *J. Chem. Soc., Chem. Commun.* **1983**, 290.

(11) A 1 mM solution of substrate in CH<sub>3</sub>CN/0.1 M tetrabutylammonium perchlorate, Pt wire electrode. The carboxylic acids were examined as their tetrabutylammonium carboxylates. The CV's are supplied in the supplementary material.

(12) Mann, C.; Barnes, K. "Electrochemical Reactions in Non-Aqueous Systems"; Marcel Dekker: New York, 1970.

(13) It was unfortunately not possible to obtain a CV on another model, glycine carboxylate, due to electrode passivation. This was only partially overcome in the case of ACC and AIB, where freshly oxidized (HNO<sub>3</sub>) and anodized (H<sub>2</sub>SO<sub>4</sub>) electrodes could be cycled only twice. Other ionic forms of ACC were inaccessible to CV due to their total insolubility in nonaqueous solvents.

(14) Substrate (100  $\mu$ mol) was oxidized in 10–15 mL of CH<sub>3</sub>CN/tetrabutylammonium perchlorate in a sealed cell by using carbon cloth electrodes. No passivation was observed.

(15) This is expected for two-electron primary amine oxidation.<sup>12</sup> As one amine is oxidized, it releases two protons, which inactivate two additional amines.

(16) The chemical yields are 0.5% based on the stoichiometry discussed above and assuming 100% current efficiency. ACC appears as the only (HPLC, NMR) basic component of the electrolyte after ion-exchange chromatography. We have been unable to isolate or identify other products thus far. Control experiments establish that the production of ethylene in primary amine oxidation (cyclohexylamine) is <2% of that in ACC oxidation.

(17) Cyanide ion was quantified using an Orion Research cyanide ion-selective electrode calibrated at cyanide concentrations from 10<sup>-6</sup> to 10<sup>-2</sup> M. Control experiments in this case also demonstrate no cyanide formation. Furthermore, cyanide is not oxidized at these potentials; cf.: Sawyer, D.; Day, R. *J. Electroanal. Chem.* **1963**, *5*, 195.

(18) Griller, D.; Ingold, K. *Acc. Chem. Res.* **1980**, *13*, 317. Sutcliffe, R.; Ingold, K. *J. Am. Chem. Soc.* **1982**, *104*, 6071.

(19) Silverman, R.; Hoffman, S.; Catus, W. *J. Am. Chem. Soc.* **1980**, *102*, 7126; *Biochem. Biophys. Res. Commun.* **1981**, *101*, 1396.

(20) McDonald, T.; Zirvi, K.; Burka, L.; Peyman, P.; Guengerich, F. *J. Am. Chem. Soc.* **1982**, *104*, 2050.

(21) Hanzlik, R.; Tullman, R. *J. Am. Chem. Soc.* **1982**, *104*, 2048.

(22) Legge, R.; Thompson, J. *Plant Cell Physiol.* **1982**, *23*, 171.

give **5**, which by  $\beta$ -fragmentation gives ethylene and cyanoformic acid **6**. Decarboxylation of **6** yields  $\text{CO}_2$ , as observed in the natural system, plus cyanide.

While the reputed<sup>3</sup> products of C1-N1 in ethylene biosynthesis are formate and ammonia, this result has never appeared in print, and one report claims that C1-N1 are widely metabolized.<sup>23</sup> Our results suggest strongly that the sequential single-electron-transfer mechanism shown above is operative for both the natural and model reactions,<sup>24</sup> and since the model system yields cyanide from C1-N1, we believe this to be good indication that cyanide is in fact produced in the natural system. Our current efforts are directed toward confirming this hypothesis.

**Acknowledgment.** I thank the Camille and Henry Dreyfus Foundation for a Research Award for New Faculty and G. M. McGeehan for performing the cyanide analysis. Professor Nathan Lewis is particularly thanked for consultation on the electrochemical aspects of this research and for access to his equipment. Dr. Deanne Snively is thanked for assistance with the FTIR spectrometer. Arnie Knudsen is thanked for a generous gift of *cis*-1,2-dideuterioethylene.

**Supplementary Material Available:** Cyclic voltammograms and infrared spectra (8 pages). Ordering information is given on any current masthead page.

(23) Burg, S.; Clagett, C. *Biochem. Biophys. Res. Commun.* **1967**, *27*, 1256.

(24) Though the yields detract somewhat from the strength of our model for a sequential single-electron-transfer mechanism, the natural system does have the advantage of sequestering its reactive intermediates in an enzyme-active site. It should also be emphasized that a chemical model that gives the highest yields of ethylene produces a stereochemical result contrary to the natural system.<sup>10</sup>

### Far-UV (185-nm) Photochemistry of Allenes: Photoisomerization and Cycloreversion Reactions of Vinylidenecyclobutane

Mark G. Steinmetz,\* Edmund J. Stark, Yao-Pin Yen, and Richard T. Mayes

Department of Chemistry, Marquette University  
Milwaukee, Wisconsin 53233

R. Srinivasan\*

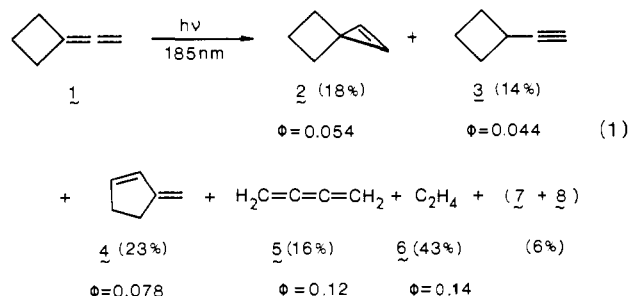
IBM Thomas J. Watson Research Center  
Yorktown Heights, New York 10598

Received July 7, 1983

The Far-UV (185 nm) solution-phase photochemistry of allenes has not been reported. Allene, which was studied under matrix isolation conditions at 8 K, photoisomerizes to cyclopropene and methylacetylene upon direct irradiation.<sup>1</sup> Contrasting behavior is provided by the vapor-phase direct photolysis of an earlier example, 1,2-hexadiene, which yields ethylene, 1,3-butadiene, and vinylcyclobutane, among other products<sup>2a</sup> However, the major far-UV photoproduct in pentane solution is 1-hexyne,<sup>3</sup> and the medium rather than the presence of an *n*-alkyl substituent appears to be controlling. A few allene  $\text{C}_3\text{H}_4$ -type photoisomerizations at long wavelengths have recently appeared; the majority are phenyl-substituted examples where the pattern of substitution must

be tailored<sup>4,5</sup> to promote rearrangement over nonproductive processes. We wish to report results of the far-UV photochemistry of vinylidenecyclobutane (**1**) which exhibits (a) photoisomerization via 1,2-C shift<sup>6</sup> to the central allenic carbon with an efficiency comparable to hydrogen migration and (b) cycloreversion to ethylene and butatriene.

The direct photolysis<sup>7</sup> of 0.033 M solutions of vinylidenecyclobutane (**1**)<sup>8</sup> in deoxygenated pentane or heptane at 185 nm produces spiro[2.3]hex-1-ene (**2**), ethynylcyclobutane (**3**), and 3-methylenecyclopentene (**4**) in yields, as a percentage of allene reacted at 14% conversion, summarized in eq 1. Products 2-4



were isolated by preparative GC<sup>9a</sup> and identified by comparison to spectral data reported in the literature for **3**<sup>10</sup> and **4**;<sup>11</sup> spirocyclopropene **2** was independently synthesized.<sup>12</sup> Highly volatile products were identified by GC<sup>9b,13</sup> as butatriene, ethylene, 1,3-butadiene (**7**), and vinylacetylene (**8**). These were isolated from the photolysate by distillation in vacuo into a trap system with the first trap at  $-78^\circ\text{C}$  and the second, containing heptane or  $\text{CCl}_4$ , at  $-196^\circ\text{C}$ . NMR analysis<sup>13</sup> of the contents of the second trap confirmed the presence of vinylacetylene and 1,3-butadiene, as well as butatriene. Purified solutions of butatriene were then obtained by purging with nitrogen to remove all ethylene and most of the butadiene and vinylacetylene as shown by NMR, GC,<sup>9b</sup> and GC-MS.

Plots of product concentration vs. time (Figure 1) clearly show that **2-4**, butatriene, and ethylene are primary products whereas the other volatiles, 1,3-butadiene and vinylacetylene, are secondary photoproducts, most likely of butatriene. Butatriene is rapidly converted to 1,3-butadiene and vinylacetylene upon direct irradiation (185 + 254 nm) in heptane. A butatriene to vinylacetylene photoisomerization under matrix isolation conditions has been reported.<sup>1</sup>

Quantum yields (eq 1) were determined from the initial slopes of concentration vs. time plots, using as an actinometer the *cis*

(4) Steinmetz, M. G.; Mayes, R. T.; Yang, J.-C. *J. Am. Chem. Soc.* **1982**, *104*, 3518.

(5) Klett, M. W.; Johnson, R. P. *Tetrahedron Lett.* **1983**, 2523.

(6) An isotope labeling experiment is as yet needed to distinguish between carbon and hydrogen migration in 1,2-cyclononadiene photochemistry ( $\lambda > 220\text{ nm}$ ): Stierman, T. J.; Johnson, R. P. *J. Am. Chem. Soc.* **1983**, *105*, 2492.

(7) The photolysis apparatus consisted of an Osram HNS 10-W/U OZ low-pressure mercury resonance lamp inside the cavity of a Suprasil immersion well apparatus of 33-mL volume for the photolysate in an ice bath. The light source gives 185- and 254-nm light.

(8) Suvorova, G. N.; Komendantov, M. I. *J. Org. Chem. USSR (Engl. Transl.)* **1979**, *15*, 1280.

(9) (a) Preparative GC separation used a 16 ft  $\times$  1/4 in. stainless steel column of 15% OV-101 on 100/120 Supelcoport at  $75^\circ\text{C}$ . (b) Analytical GC separations used a 10 ft  $\times$  1/8 in. glass column of 10% SP2100 on 100/120 Supelcoport at  $60^\circ\text{C}$ ; retention times for **5-8** were matched against authentic samples on two additional 10 ft  $\times$  1/8 in. columns: Porapak N at  $50^\circ\text{C}$  and 15% DOPN on 100/120 Supelcoport at  $10^\circ\text{C}$ . The FID was calibrated for the response of **1**, **2**, **6**, and **8**. Since butatriene is susceptible to polymerization,<sup>13a</sup> the response factor of **8** was used.

(10) Bruckmann, P.; Klessinger, M. *J. Electron. Spectrosc. Relat. Phenom.* **1973**, *2*, 341.

(11) Huntsman, W. D.; DeBoer, J. A.; Woosley, M. H. *J. Am. Chem. Soc.* **1966**, *88*, 5846.

(12) Yakushkina, N. I.; Bolesov, I. G. *J. Org. Chem. USSR (Engl. Transl.)* **1979**, *15*, 853.

(13) (a) Butatriene was independently synthesized: Montijn, P. P.; Brandsma, L.; Arens, J. F. *Recl. Trav. Chim. Pays-Bas* **1967**, *86*, 129. (b) Ethylene and vinylacetylene were purchased from Ideal Gas Products, Edison, NJ. (c) 1,3-Butadiene was obtained from thermolysis of 3-sulfolene and purified by an aqueous KOH was to remove  $\text{SO}_2$ .

(1) Chapman, O. L. *Pure Appl. Chem.* **1975**, 511.

(2) (a) Ward, H. R.; Karafiath, E. *J. Am. Chem. Soc.* **1969**, *91*, 7475. (b) For related examples, see ref 3.

(3) Intermediates in thermal and photochemical interconversions among allenes, cyclopropenes, and methylacetylenes have been reviewed: Steinmetz, M. G.; Srinivasan, R.; Leigh, W. J. *Rev. Chem. Intermed.* **1983**, *7*, 0000.